



# Higher Order Modeling of Reactor Regulating System and Nonlinear Neural Model Predictive Controller Design for a Nuclear Power Generating Station

Arshad H. Malik<sup>1\*</sup>, Aftab A. Memon<sup>2</sup>, and Feroza Arshad<sup>3</sup>

<sup>1</sup>Department of Maintenance Training, Pakistan Atomic Energy Commission, A-104, Block-B, Kazimablad, Model Colony, Karachi, Pakistan

<sup>2</sup>Department of Telecommunication Engineering, Mehran University of Engineering and Technology, Jamshoro, Sindh, Pakistan

<sup>3</sup>Department of Management Information System, Pakistan Atomic Energy Commission, B-63, Block-B, Kazimablad, Model Colony, Karachi, Pakistan

**Abstract:** In the existing instrumentation and control system of an operating Pressurized Heavy Water Reactor (PHWR) based nuclear power plant, conventional controllers are used to control the reactor power. A new idea of Nonlinear Neural Model Predictive Controller (NNMPC) is introduced in this research work. The new 17th order nonlinear higher order model of Reactor Regulating System (RRS) is developed under different plant operating modes and various parametric conditions in Single Input Multi Output (SIMO) configuration with special emphasis on Helium Control Valve Dynamics (HCVD) and Coupled Nonlinear Iodine and Xenon Dynamics (CNIXD). The SIMO RRS model is developed based on first principle. The 17th order model is reduced to 9th order lower dynamic model using Balanced Truncation Method (BTM). The Reduced Order SIMO RRS (RO-SIMO-RRS) model is programmed, simulated and validated in SIMULINK environment. The plant Neural SIMO RRS (N-SIMO-RRS) model is developed using innovative data generated from RO-SIMO-RRS simulations. The plant neural N-SIMO-RRS model is optimized using Levenberg-Marquardt Algorithm (LMA). Using the identified N-SIMO-RRS model, the Nonlinear Neural Model Predictive Controller (NNMPC) is designed, trained, verified, validated, and finally optimized using the backtracking technique in the SIMULINK environment. The optimized results are obtained from designed closed loop RRS and found within the acceptable design limits. The performance of the proposed closed loop RRS is also tested in reference tracking mode with excellent fast tractability near the optimal target demanded power level.

**Keywords:** SIMO Modelling, Reactor Regulating System, Model Reduction, Nonlinear Neural Predictive Control, Helium Control Valve Dynamics, PHWR, Nuclear Power Plant

## 1. INTRODUCTION

In this research work, a Pressurized Heavy Water Reactor (PHWR) type nuclear power plant system is focused which is associated with reactor power control system known as Reactor Power Regulating System (RPRS) or simply Reactor Regulating System (RRS) [1].

A robust H-Infinity controller has been designed for current PHWR in [2] which is also under consideration in this research. A state space

based Model Predictive Controller (MPC) has been designed for reactor power control systems for a different Pressurized Water Reactor (PWR) type nuclear power generating station in [3]. A data driven composite MPC has been captured for current PHWR Reactor Power Controller (RPC) in [4]. A nonlinear higher order model of RRS of operating PHWR type nuclear power generating station has been developed in [5] and Linear Matrix Inequalities (LMI) based Fast Output Sampling (FOS) controller has been designed. The higher order dynamics of an Advanced Heavy

Water Reactor (AHWR) have been reduced using Balanced Truncation Method (BTM) under reactor transient conditions for controller design purposes in [6]. A Genetic Algorithm (GA) tuned Proportional Integral Derivative (PID) controller has been designed for reactor kinetics of PWR in [7]. A fuzzy PID controller has been identified for PWR in load following mode in [8]. A robust H-Infinity mixed sensitivity controller has been proposed for small PWR with parametric uncertainties in [9]. A robust Linear Quadratic Gaussian (LQG) controller has been synthesized for the PWR type nuclear power plant [10]. A Multi-Layer Perceptron compensated output feedback PD controller has been designed for Gas Cooled Reactor (GCR) in [11]. A neural network based MPC has been designed for Single Input Single Output (SISO) power converter in [12]. A reactor power change constrained based fuzzy logic controller has been designed for a nuclear research reactor in [13]. A fuzzy logic-based MPC controller has been designed for the reactor power control of the PWR type nuclear power plant [14]. A decentralized fuzzy MPC has been proposed for PWR with xenon dynamics in [15]. A MLP based model free MPC has been designed for nuclear steam supply system in [16].

In this research work, a new multi-objective optimized Single-Input Multi-Output (SIMO) Nonlinear Neural Network based Model Predictive Controller (NNMPC) SIMO-NNMPC is proposed

for a Novel Full Higher Order Integrated SIMO Reactor Regulating System (NFHOI-SIMO-RRS) and Reduced Order SIMO RRS (RO-SIMO-RRS) models with special emphasis on Helium Control Valve Dynamics (HCVD) and Coupled Nonlinear Iodine and Xenon Dynamics (CNIXD). The proposed NNMPC is designed, for the first time, for PHWR type nuclear power generating station with substantially reduced online computational requirements as compared to conventional MPC techniques. The computational effort involved in the NNMPC training depends mainly on the artificial neural network complexity, and not on the length of the control horizon. This makes it feasible to design a controller with a longer control horizon.

## 2. MATERIALS AND METHODS

### 2.1 Reactor Regulating System

SReactor Regulating System (RRS) is designed to regulate the reactor power. RRS is a fine reactivity control system using Helium Gas (HG) Control Valve (CV) as modulating element. In RRS, there are two power channels known as Regulating Channel-A and Regulating Channel-B respectively. Both channels act like redundant systems. There are two Helium Gas Control Valves (HGCV1 and HGCV2) installed between the upper and lower Calandria in PHWR type CANDU Nuclear Power Plant [1].

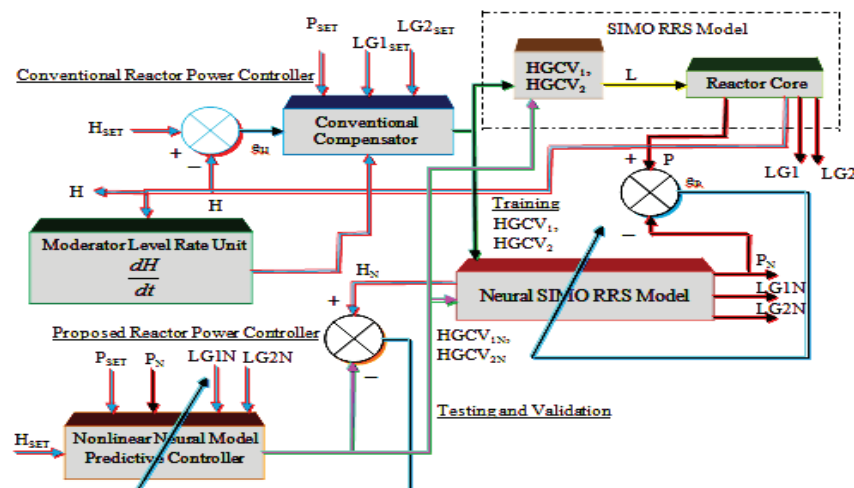


Fig. 1. Closed loop design architecture of existing and proposed RRS.

## 2.2 Existing Reactor Power Controller

Two Reactor Power Controllers (RPC) control Regulating Channel-A and Regulating Channel-B. At a time, reactor power is controlled by one RPC while second RPC works as Backup Controller in tracking mode. The existing controller is a digital controller known as AC132 controller. The reactor power is normalized and expressed in %. In this research paper, the plant operation is considered in Reactor Following Mode (RFM) also known as Neutron Power Mode (NP-Mode). In RFM, there are four set points designated as moderator level set point (HSET), reactor power set point (PSET), logarithmic of reactor power set point (LG1SET) and rate of change of logarithmic of reactor power set point (LG2SET). Similarly, there are four corresponding measured variables designated as moderator level (H), reactor power (P), logarithmic of reactor power (LG1) and rate of change of logarithmic of reactor power (LG2). Therefore, four sub controllers will be considered for design and analysis, in detail, in subsequent sections. RPC is basically a conventional compensator technology implemented on Programmable Logic Controllers (PLCs) [1]. The closed loop architecture of existing RRS is shown in Fig.1.

## 2.3 Proposed Reactor Power Controller

The proposed reactor power controller is basically Nonlinear Neural Model Predictive Controller (NNMPC). Therefore, two major milestones are required to achieve in this research work. Firstly, a Neural SIMO RRS (N-SIMO-RRS) model is required to develop for NNMPC. Such a N-SIMO-RRS model is extracted from Reduced Order SIMO-RRS (RO-SIMO-RRS) model using data driven technique. RO-SIMO-RRS model is developed after implementing dimension reduction technique on Full Higher Order SIMO-RRS (FHO-SIMO-RRS) model. The closed loop architecture of proposed RRS is shown in Fig.1.

NNMPC1 consists of N-SIMO-RRS model and the optimizer. The optimizer computes controller signal  $u^*$  that minimizes the controller cost function  $J_C$  which is given as [16]:

$$J_C = Y(t) - \rho U(t) \quad (1)$$

Where

$$U(t) = \sum_{j=1}^{N_u} (u'(t+j-1) - u'(t+j-2))^2$$

$$Y(t) = \sum_{j=N_1}^{N_2} (y_r(t+j) - y_m(t+j))^2$$

Where  $N_1$ ,  $N_2$  and  $N_u$  define the minimal and maximal prediction horizons of controlled output of RO-SIMO-RRS and prediction horizon of controller signal. The  $u^*$  is the predicted NNMPC controller signal,  $y_r$  is the desired response of RO-SIMO-RRS model and  $y_m$  is the network model response of N-SIMO-RRS model. The  $\rho$  value determines the contribution of the sum of the squares of the control increments that has an impact on the performance index.

Since, four sub controllers are configured for  $H$ ,  $P$ ,  $LG1$  and  $LG2$  separately in SISO form for HGCV1, therefore, four separate cost functions are defined against the same input  $L$  as:

$$J_{C11} = Y_{11}(t) - \rho_{11} U_{HGCV1}(t) \quad (2)$$

$$J_{C12} = Y_{12}(t) - \rho_{12} U_{HGCV1}(t) \quad (3)$$

$$J_{C13} = Y_{13}(t) - \rho_{13} U_{HGCV1}(t) \quad (4)$$

$$J_{C14} = Y_{14}(t) - \rho_{14} U_{HGCV1}(t) \quad (5)$$

The structure of neural MPC of reduced order plant model is shown in Fig. 2.

Similarly, cost functions are designed for HGCV2. Constraints are imposed on input, change in input, output and change in output for each sub controllers for HGCV<sub>1</sub> and HGCV<sub>2</sub>.

## 2.4 Nonlinear Neural MPC Optimization

### 2.4.1 Backtracking Technique

A one-dimensional (1D) linear cost function minimization technique that works on a linear search algorithm is called backtracking. It uses step multiplier and backtracks, till the quadratic approximation of controller cost function which is a function of step multiplier and current point is minimized in the search direction. If the quadratic approximation based cost function is not sufficiently reduced then a cubic approximation is used and

minimized.

### 2.4.2 Stopping Criteria

When training of NNMPC is accomplished with minimum error then this represents that the maximum number of iterations (epochs) reached. Minimum mean square error of the epoch is the square root of the sum of squared differences between the NNMPC predicted outputs and actual existing RPC outputs divided by the number of training samples of controller.

## 2.5 NewNonlinear Higher Order Dynamics of SIMO RRS Model

### 2.5.1. Choice of Reference Model

The reference model is adopted from an already conducted and established research [5] which is a Single Input and Multi-Output RRS model that includes Nuclear Reactor Dynamics (NRD) and Helium Control Valve Dynamics (HCVD) in electrical form for reactivity management for the current PHWR under consideration. The assumptions taken into account for higher order modelling as reference model are that six precursor groups are chosen, reactor power is only controlled by Helium control valves and moderator level is not entered in the band of reactor regulating control rods. This non-linear 15<sup>th</sup> order SIMO-RRS model is linearized and transformed into state equation model form as [5]:

$$\dot{x}(t) = Ax(t) + Bu(t) \quad (6)$$

$$y(t) = Cx(t) \quad (7)$$

where  $A \in R^n$ ,  $B \in R^m$  and  $C \in R^p$  are the matrices of appropriate dimensions.

### 2.5.2. Coupled Nonlinear Iodine and Xenon Dynamics

In a reactor power system, nuclear fission reactions take place. In nuclear reactions, fission fragments are produced and all fission products absorb neutrons to some extent, so are known as reactor poisons. Most fission product poisons simply build up slowly as the fuel burns up and are accounted for as a long-term reactivity. The neutron absorbing fission products Xenon-135 and Samarium-149 have particular operational importance. Their concentrations can change quickly, produces major changes in neutron absorption on a relatively short time scale. Each arises from the decay of a precursor fission product, which controls their production rate, but, because they have large absorption cross-sections, their removal changes quickly with changes in thermal neutron flux  $\phi_r$ .

Xenon-135 (often simply referred to just as xenon) is the most important fission product poison. It has a very large absorption cross-section and high production rate.

Xenon is a strong neutron absorber so its presence in the fuel creates a large negative reactivity in the core. The reactivity worth of the Xe-135 is known as the Xenon load. Therefore, the relationship between Xenon load and reactor power is inverse, as the Xenon load increases, the reactor power decreases. Similarly, the iodine load is the

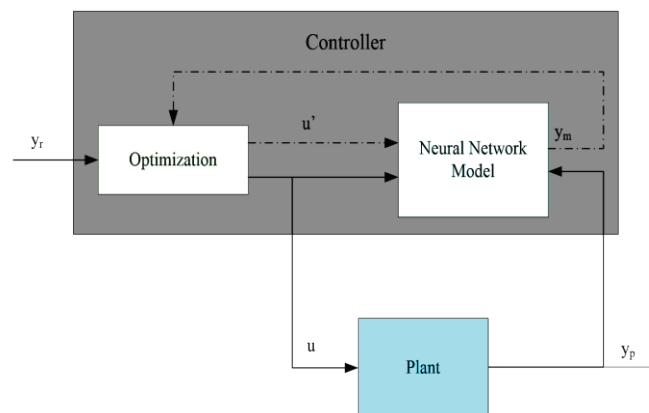


Fig. 2. Structure of neural MPC of reduced order plant model.

reactivity that it would insert into the reactor, if all the iodine present suddenly changes into xenon [1].

Iodine dynamics is represented by the following expression in PHWR [15]:

$$\frac{dI(t)}{dt} = \gamma_I \Sigma_f \phi_T - \lambda_I I - \sigma_{aI} I \quad (8)$$

Where I is the concentration of I-135 (atoms/cm<sup>3</sup>),  $\gamma_I$  is the effective yield of I-135 (atoms per fission),  $\Sigma_f$  is the thermal fission cross-section,  $\phi_T$  is the reactor neutron flux,  $\lambda_I$  is the decay constant for I-135, and  $\sigma_{aI}$  is the I-135 absorption cross-section.

Xenon dynamics is represented by the following expression in PHWR [15]:

$$\frac{dX(t)}{dt} = \gamma_X \Sigma_f \phi_T + \lambda_I I - \lambda_X X - \sigma_{aX} \phi_T X \quad (9)$$

Where X is the concentration of Xe-135,  $\gamma_X$  is the effective yield of Xe-135,  $\lambda_X$  is the decay constant for Xe-135, and  $\sigma_{aX}$  is the absorption cross-section for Xe-135.

The thermal flux and reactor power are correlated by the following expression for an operating PHWR[1]:

$$\phi_T = p(\%) \times \frac{137MWe}{100} \times 3.12 \times 10^{10} \frac{\text{fissions}}{\text{watt.sec}} \times \frac{1}{\Sigma_f V} \quad (10)$$

### 2.5.3 Integrated SIMO RRS Model

The nonlinear poison model of 2nd order developed in this research work is then linearized and integrated with already developed linearized 15th order SIMO RRS model. The new Higher Order Integrated SIMO-RRS (HOI-SIMO-RRS) model is highly precise and state of the art.

Now, the continuous time state space model of SIMO-RRS expressed equations (6) and (7) is appended with Xenon poison dynamics. The appended higher order model is then restructured for Helium Control Valve Dynamics (HCVD) and transformed into non-electrical form and finally represented in state space form as:

$$\dot{x}(t) = A_{AR} x(t) + B_{AR} u(t) \quad (11)$$

$$y(t) = C_{AR} x(t) \quad (12)$$

Where  $A_{AR} \in R^r$ ,  $B_{AR} \in R^m$  and  $C_{AR} \in R^p$  are the appended and restructured matrices of appropriate dimensions ( $r > n$ ).

The integrated appended dimensionality of input vectors for both control valves in the proposed design  $17 \times 1$ .

The input vector, state vector and output vector of a PHWR model described in equations (6) and (7) are as follows:

$$u(t) = L$$

$$x(t) = [\delta P \ \delta \bar{C} \ \delta L \ \delta \bar{G}_{12} \ \delta \bar{R}_{12} \ \delta \bar{L} \ \delta Q_M \ \delta \bar{X}_I]^T$$

Where

$$\delta \bar{C} = [\delta C_1 \ \delta C_2 \ \delta C_3 \ \delta C_4 \ \delta C_5 \ \delta C_6]^T$$

$$\delta \bar{G}_{12} = [\delta LG1 \ \delta LG2]^T$$

$$\delta \bar{L} = [\delta L_1 \ \delta L_2]^T$$

$$\delta \bar{X}_I = [\delta X \ \delta I]^T$$

$$y(t) = [y_1 \ y_2 \ y_3 \ y_4]^T = [H \ P \ LG1 \ LG2]^T$$

where H, P, LG1 and LG2 are moderator level, power, log power and rate log power respectively.

### 2.5.4 Reduced Order SIMO RRS Model

The 17<sup>th</sup> order SIMO RRS model is reduced by Balanced Truncation Method [6] and the Reduced 9<sup>th</sup> Order SIMO RRS (RO-SIMO-RRS) model is obtained from equations (11) and (12) based on optimal value of tolerance value of error bound for RO-SIMO-RRS model as:

$$\dot{x}(t) = A_R x(t) + B_R u(t) \quad (13)$$

$$y(t) = C_R x(t) \quad (14)$$

where  $A_R \in R^d$ ,  $B_R \in R^m$  and  $C_R \in R^p$  are the matrices

of appropriate dimensions ( $d < r$ ).

The input vector, state vector and output vector of RO-SIMO-RRS model described in equations (13) and (14) are as follows:

$$u(t) = L$$

$$x(t) = [\hat{\alpha}x_1 \ \hat{\alpha}x_2 \ \hat{\alpha}x_3 \ \hat{\alpha}x_4 \ \hat{\alpha}x_5 \ \hat{\alpha}x_6 \ \hat{\alpha}x_7 \ \hat{\alpha}x_8 \ \hat{\alpha}x_9]^T$$

$$y(t) = [y_1 \ y_2 \ y_3 \ y_4]^T = [H \ P \ LG1 \ LG2]^T$$

Where H, P, LG1 and LG2 are moderator level, power, log power and rate log power respectively. The error bound for RO-SIMO-RRS model in frequency domain is defined as:

$$\|G_{RO-SMO-RRS}(s) - G_{HOI-SMO-RRS}(s)\| = \varepsilon \quad (15)$$

Where  $\varepsilon$  is tolerance value.

## 2.6 Neural SIMO RRS Model

### 2.6.1 Choice of Neural Inputs and Outputs

Assuming for HGCV<sub>1</sub>, the dataset  $D_i$  contains  $Q$  number of data patterns and  $d_i$  is an  $(n_u + n_r)$  dimensional vector containing  $n_u$  number of inputs and  $n_r$  number of outputs defined as:

$$d_i = \{u_{HGCV1}, t_P, t_H, t_{LG1}, t_{LG2}\}$$

Similarly, assuming for HGCV<sub>2</sub>, the dataset  $D_j$  contains number of data patterns and  $d_j$  is an  $(n_u + n_r)$  dimensional vector containing  $n_u$  number of inputs and  $n_r$  number of outputs defined as:

$$d_j = \{u_{HGCV2}, t_P, t_H, t_{LG1}, t_{LG2}\}$$

### 2.6.2 Optimization of N-SIMO-RRS Model

N-SIMO-RRS model is divided into four sub N-SISO-RRS models. N-SISO1-RRS, N-SISO2-RRS, N-SISO3-RRS and N-SISO4-RRS sub models are optimized in distributed parallel computing fashion using standard Levenberg-Marquardt algorithm implemented in MATLAB.

### 2.6.3 Formulation of MSE for N-SIMO-RRS Model

Now, if where  $t_{nt}$  is the desired outputs of SIMO-RRS model for each input pattern and  $y_{nt}$  is the actual

output produced by each N-SISO-RRS model, then Mean Square Error (MSE) is a dimensionless value computed to deduce the N-SISO-RRS model performance for training, testing and validation for each  $n_r$ .

For moderator level (H), MSEs can be defined as:

$$MSE_{Training} = \sum_{q=1}^{Q_{tr}} (t_1 - y_1)^2 = \sum_{q=1}^{Q_{tr}} (H - H_N)^2$$

$$MSE_{Testing} = \sum_{q=1}^{Q_{te}} (t_1 - y_1)^2 = \sum_{q=1}^{Q_{te}} (H - H_N)^2$$

$$MSE_{Validation} = \sum_{q=1}^{Q_{va}} (t_1 - y_1)^2 = \sum_{q=1}^{Q_{va}} (H - H_N)^2$$

Similarly, all rest of the MSEs can be defined for P, LG1 and LG2.

The structure of N-SIMO-RRS model for training, testing and evaluation is shown in Fig. 2.

## 3. RESULTS AND DISCUSSION

The simulations and analysis of 15<sup>th</sup> order SIMO-RRS model described in equations (1) and (2) were discussed in detail in [5]. Now, in this research work, a new addition of coupled dynamics of Iodine and Xenon described in equations (8), (9) and (10) are modeled in Simulink environment in MATLAB as shown in Fig. 3. This model is very useful for long term dynamic studies of nuclear reactor dynamics. All the constants and parameters are properly modeled for dynamic analysis purposes. The impact of Xenon dynamics is considered and integrated with reference model [5].

Basically, the Xenon dynamics is highly nonlinear in nature and helpful for power dynamics on large time-scale, especially in power transients. The power transient consists of reactor power maneuvering in either direction depending on the power demand changes.

### 3.1 Estimation and Implementation of RO-SIMO-RRS

The new 17<sup>th</sup> order SIMO-RRS (HOI-SIMO-RRS) model is reduced using BTM in MATLAB



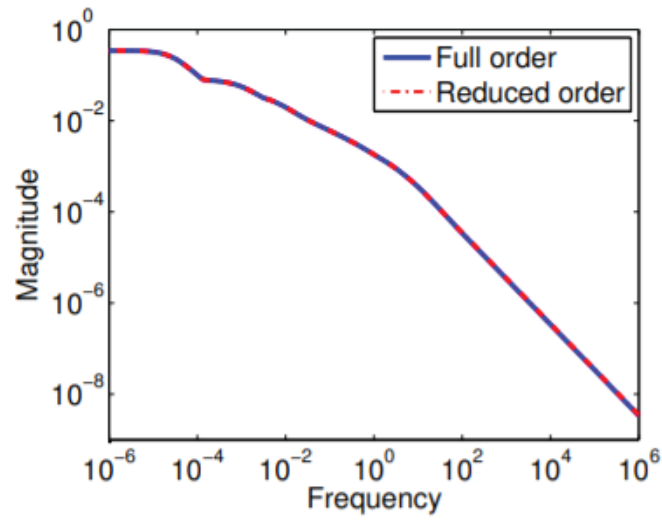


Fig. 4. Comparison of frequency responses of HOI- SIMO-RRS and RO-SIMO-RRS models.

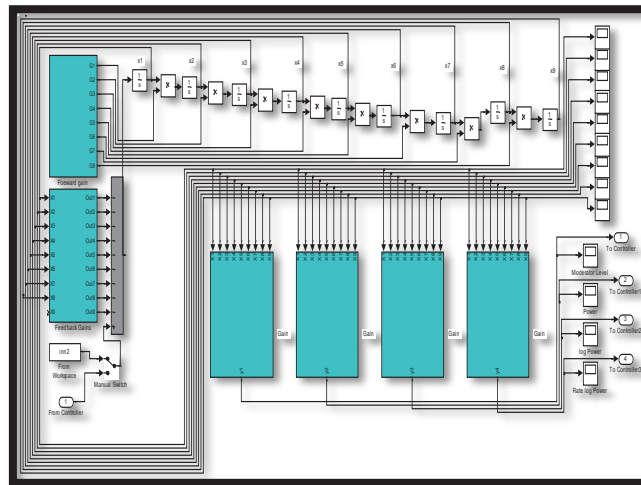


Fig. 5. Simulink model of RO-SIMO-RRS model

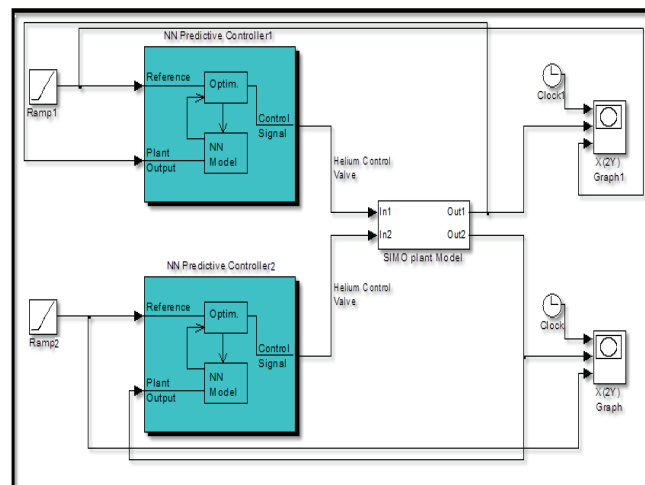


Fig. 6. Configuration of redundant NN MPC-1 and NN MPC-2 interfaced with RO-SIMO RRS model

**Table 1.** Parameters of N-SIMO-RRS model

Parameters	Design Values
Number of Input ( $n_u$ )	1
Number of Outputs( $n_r$ )	4
No of hidden layers	9
No of neurons in hidden layer ( $n_h$ )	25
Sampling Interval (seconds)	0.16
Total Samples ( $Q$ )	9000
Training Samples ( $Q_{tr}$ )	5400
Testing Samples ( $Q_{te}$ )	1800
Validation Samples ( $Q_{va}$ )	1800
Mu Value ( $\mu$ )	0.0001
Training Epochs	200
Performance	$1.8 \times 10^{-6}$

Four sub controllers NNMPC11, NNMPC12, NNMPC13 and NNMPC14 are configured in distributed parallel computing framework in Simulink environment using equations (2) to (5). The parameters of designed sub controller of NNMPC11 for moderator level are tabulated in Table (2) for reference purposes.

**Table 2.** Parameters of NNMPC11 for moderator level

Parameter Name	Design Value
Minimal Cost Horizon (N1)	1
Maximal Cost Horizon (N2)	7
Control Horizon (Nu)	2
Control Weighting Factor ( $\rho_{11}$ )	0.1
Search Parameter ( $\alpha_{11}$ )	0.02
Iterations per sample time	2

Similarly, the design parameters of rest of three sub controllers NNMPC12, NNMPC13 and NNMPC14 for HGCV1 and four sub controllers NNMPC21, NNMPC22, NNMPC23 and NNMPC24 HGCV2 are evaluated in NP-mode.

### 3.3 Closed Loop Simulation Scenarios for Validation of Proposed NNMPC

Two case studies are considered in this research work that shall be discussed in the subsequent sections.

#### 3.3.1 Rule based Reactor Power Rising Scenario from 0% to 75%

In this first case study, reactor power rising transient is considered with RO-SIMO-RRS model

and NNMPC. The reactor power is increased from 0% to 75% as per procedure as laid down in [1]. This procedure is known as rule based transient in engineering language. The rule base scenario is a predefined combination of steps, ramps, checks, permissives and interlocks. The behaviour of Helium control valve controller and corresponding changes in moderator level, reactor power, logarithmic reactor power and rate of logarithmic reactor power are simulated and analyzed as shown in Fig.7 to Fig. 11 respectively.

All the parametric behavior is well controlled and well within the design constraints imposed on closed loop RRS [1, 5]. The Helium control valve signal is observed highly nonlinear in nature and remained within 100% throughout the power rising transient. The moderator level rises from 35 inches to 175 inches which is well within 190 inches control limit. The reactor power increases from 0% to 75% without any overshoot which is one of most important design basis of RRS[1, 5]. The logarithmic reactor power is quite well because rate of logarithmic reactor power is within 4%RP/sec design limit.

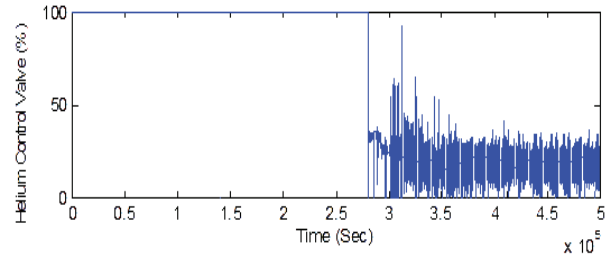


**Fig. 7.** Helium control valve controller signal during power rising transient.

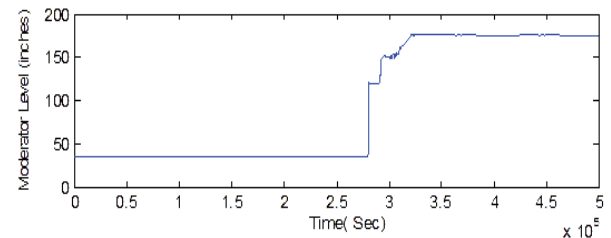


**Fig. 8.** Moderator level during power rising transient.

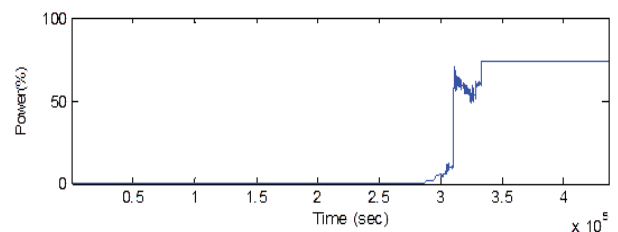


**Fig. 9.** Reactor power during power rising transient.

### 3.3.2 Reactor Power Rising Scenario from 0% to 50% in Reference Tracking Mode

In this second case study, reactor power rising transient is considered with HOI-SIMO-RRS model and NNMPC in reference tracking mode. In this mode, plant is to follow the reference command signal which is implemented as per plant design procedure. Such design studies are carried with any of the redundant channel that replicates the actual plant operating configuration. The proposed NNMPC is configured with HOI-SIMO-RRS model as shown in Fig. 12.

The reactor power is increased from 0% to 50% in reference tracking mode in NP-mode. This procedure is known as ramp transient in engineering language. The behavior of HOI-SIMO-RRS model with special emphasis on Xenon

dynamics, the behavior of Iodine concentration, Xenon concentration, moderator level as a result of Helium control valve controller signal variation and corresponding changes in reactor power are simulated and compared with reference signal as patent ramp transient as shown in Fig. 13 to Fig. 16 respectively. All the parametric behavior is well controlled and well within the design constraints imposed on closed loop RRS in reference tracking mode in a reactor following transient.

There is no overshoot observed in any of the parameter. Moderator level and reactor power as key parameters of interest are observed smooth and fast with leading dynamics and reached the target moderator level of 175 inches and reactor power of 50%. The moderator level is found within design limits even with Xenon load. Hence, the proposed closed loop SIMO-RRS is sufficiently stable and found robust in reference tracking mode.

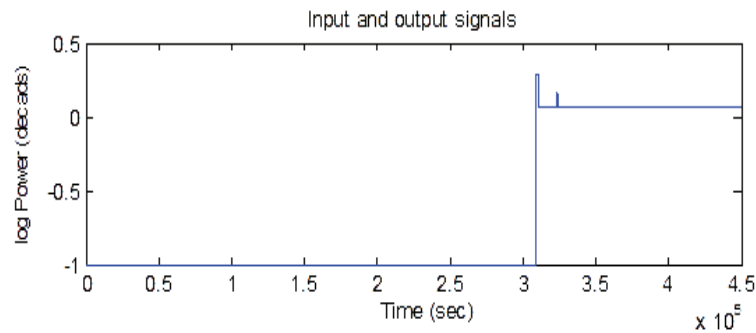


Fig. 10. Log reactor power during power rising transient.

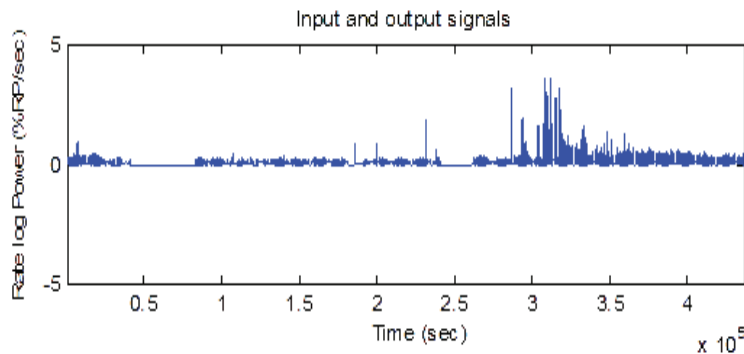


Fig. 11. Rate log reactor power during power rising transient.

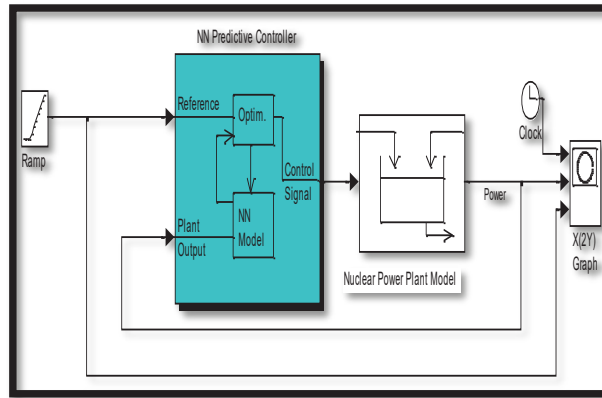


Fig. 12. Structure of NN MPC interfaced with HOI-SIMO-RRS model.

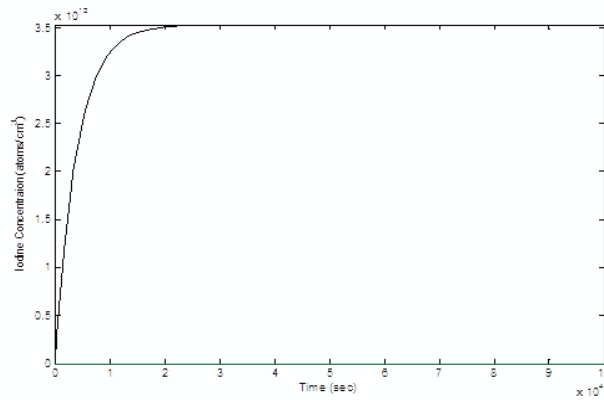


Fig. 13. Variation of Iodine concentration in reference tracking mode.

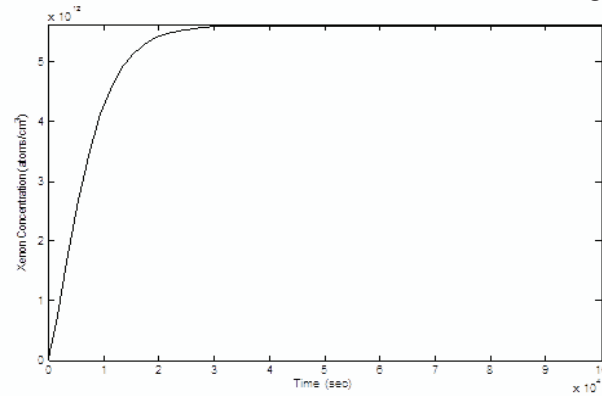


Fig. 14. Variation of Xenon concentration in reference tracking mode.

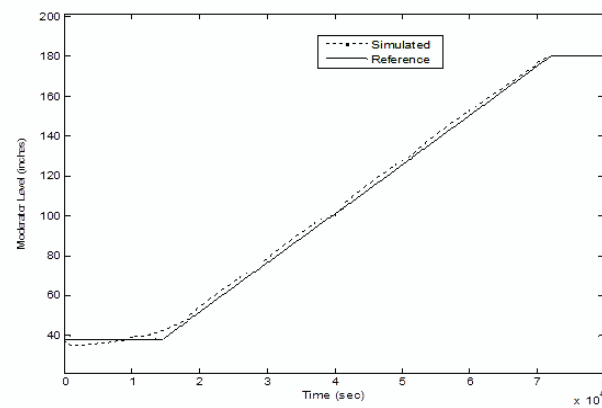
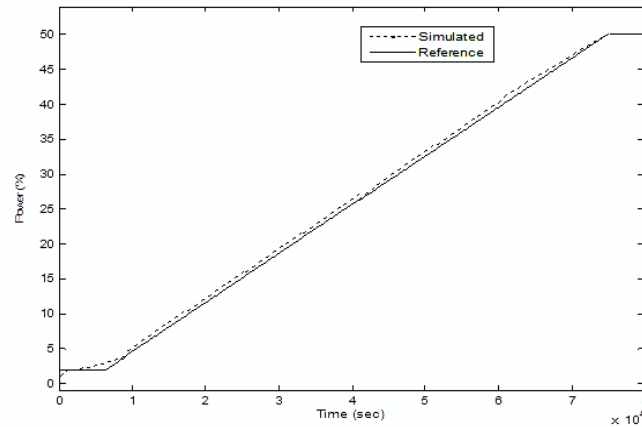


Fig. 14. Performance of proposed closed loop RRS moderator level in reference tracking mode.



**Fig. 16.** Performance of proposed closed loop RRS reactor power in reference tracking mode.

#### 4. CONCLUSIONS

In this research work, a new nonlinear neural model predictive controller has been designed as new innovative replacement of conventional compensator of RRS. The performance of NNMPC has been tested and evaluated with RO-SMO-RRS model under rule based reactor power transient and with HOI-SIMO-RRS model under reference tracking mode and found smooth, faster and robust in closed loop configuration. All the parametric trends prove that the proposed closed loop SIMO-RRS model with NNMPC is realistic and within design bounds.

#### 5. ACKNOWLEDGEMENTS

The support of the Pakistan Atomic Energy Commission, Chashma Centre of Nuclear Training and Computer Development Division of KANUPP is gratefully acknowledged.

#### 6. REFERENCES

1. A. H. Malik. Nuclear reactor instrumentation and control. *KINPOE, PAEC, Pakistan* (2017).
2. A. H. Malik,, A. A. Memon, and M. R. Khan. Synthesis of model based robust stabilizing reactor power controller for nuclear power plant. *Mehran University Research Journal of Engineering and Technology* 30 (2): 265-276 (2011).
3. W. Guoxu, B. Zeng, Z. Xu., W. Wu. and X. Ma. State-space model predictive control method for core power control in pressurized water reactors nuclear power stations. *Nuclear Engineering and Technology* 49 (1): 134-140 (2017).
4. A. H. Malik,, A. A. Memon, and M. R. Khan. Synthesis of reference tracking multivariable composite controller for PHWR. *Proceedings of Pakistan Academy Sciences* 47 (4): 245-252 (2010).
5. A. H. Malik, A. A. Memon, and M. R. Khan. Dynamic modeling and controller design for nuclear power plant. *Journal of Engineering and Applied Sciences* 29 (2): 19-33 (2010).
6. R. S. Ananthoju, E. Tiwari, A. P. and M. N. Belur. Model Reduction of AHWR space time kinetics using balanced truncation. *Annals of Nuclear Energy* 102: 454-464 (2017).
7. S. M. H. Mousakazemi. Comparison of error-integral performance indexes in a GA-tuned PID controlling system of a PWR-type nuclear reactor point-kinetics model. *Progress in Nuclear Energy* 132: 1412-1423 (2021).
8. Z. Wenjie, Q. Jiang, Jinsen X. and T. Yu. A functional variable universe fuzzy PID controller for load following operation of PWR with the multiple model. *Annals of Nuclear Energy* 140: 1-6 (2020).
9. X. Y. Pengfei, P. Wang, J. Qing, S. Wu and F. Zahao. Robust power control design for small pressurized water reactor using H infinity mixed sensitivity method. *Nuclear Engineering and Technology* 52: 1443-1451 (2020).
10. V. Vajpayee, V. Becerra, N. Bausch, J. Deng, S. R. Shimjith and A. J. Arul. Robust-optimal integrated control design technique for pressurized water-type nuclear power plant. *Progress in Nuclear Energy* 131: 1-14 (2021).
11. Zhe, D. An artificial neural network compensated output feedback power control for modular high temperature gas-cooled reactors. *Energies* 07: 1149-

- 1170 (2014).
12. S. Sanaz, R. Heydari., M. Mohiti., M. Savaghebi. and J. Rodriguez. Model-free neural network-based predictive control for robust operation of power converter. *Energies* 14: 01-12 (2021).
  13. S. M. Mohd, N. A. M. Subha., F. Hassan., and A. Ahmad. Application of fuzzy logic for power change rate constraint in core power control at reactor TRIGA PUSPATI. *IOP Conference Series: Material Science and Engineering* 785: 1-18 (2020).
  14. L. Xiangjie, and M. Wang. Nonlinear fuzzy model predictive control for a PWR nuclear power plant. *Mathematical Problems in Engineering* 2014: 1-10 (2014).
  15. L. Xiangjie, Di. Jiang., and K. Y. Lee. Decentralized fuzzy MPC on special power control of a large PHWR. *IEEE Transactions on Nuclear Science* 63 (4): 1-10 (2016).
  16. Z. Dong, Z. Zhang., Y. Dong., and X. Huang. Multi-layer perception based model predictive control for thermal power of nuclear superheated-steam supply systems. *Energy* 151: 116-125 (2018).

